Formation of cashew gum thin films onto silicon wafers or amino-terminated surfaces and the immobilization of Concanavalin A on them

Jeanny da S. Maciel [a], Priscila M. Kosaka [b], Regina C.M. de Paula [a], Judith P.A. Feitosa [a], Denise F.S. Petri [b,*]

[a] *Universidade Federal do Ceará, Departamento de Química Orgânica e Inorgânica, P.O. Box 12200, 60455-760 Fortaleza, CE, Brazil*
[b] *Universidade de São Paulo, Instituto de Química, P.O. Box 26077, 05513-970, São Paulo, SP, Brazil*

Abstract

The adsorption behavior of cashew gum (CG), a galactose-rich polysaccharide, onto silicon wafers and amino-terminated surface was investigated by means of ellipsometry, atomic force microscopy (AFM) and contact angle measurements. The pH has a strong influence on the adsorption behavior. At pH values lower than 4 amino-terminated surfaces are positively charged and CG behaves as a polyanion, due to the glucuronic acid units along its chain. Under acidic conditions, adsorption was driven by electrostatic forces, following the screening-reduced adsorption regime. The adsorption constant (K_{ads}) of CG onto amino-terminated surfaces was determined as 2.5×10^5 L mol^{-1}. At pH 6 the adsorption of CG onto bare Si wafers was less favored, indicating that silanol groups (Si–OH) and many negative charges (Si–O$^-$) on the substrate repel the negatively charged CG segments. On the other hand, hydrogen bonding between silanol groups and sugar hydroxyl groups might drive the adhesion of CG onto Si wafers. CG layers deposited onto amino-terminated substrates or Si wafers are hydrophilic and smooth.

The adsorption of Concanavalin A (Con A), a mannose and glucose specific lectin, onto CG-covered amino-terminated surfaces increased with Con A concentration, indicating cooperativity effect. On the contrary, the adsorption of Con A onto Si wafers could be fitted with the Langmuir adsorption model, yielding K_{ads} $(2.0 \pm 0.2) \times 10^6$ L mol^{-1}. This result evidenced that although CG is predominantly composed of galactose, the presence of glucose (14%) as side-chain favors the interaction with Con A.
© 2007 Elsevier Ltd. All rights reserved.

1. Introduction

The adsorption of polysaccharides onto solid substrates provides an environment for the immobilization of biomolecules (Barbucci et al., 2005; Petri et al., 1999a; Sackmann, 1996; Wiegand, Jaworek, Wegner, & Sackmann, 1997). Specific interactions such as protein–substrate (Fujimoto, Reis, Petri, & Campana, 2002; Sierakowski, Freitas, Fujimoto, & Petri, 2002), antigen–antibody and lectin–carbohydrate (Castro & Petri, 2005; Castro, Kappl, & Petri, 2006; Gad, Ioth, & Ikai, 1997; Lekka, Laider, Dulinska, Labedz, & Pyka, 2004; Revell, Knight, Blyth, Haines, & Russel, 1998; Smith, Thomas, Kiessling, & Corn, 2003; Touhami, Hoffman, Vasella, Denis, & Dufrêne, 2003a) can be used with advantage for development of biosensors (Castro et al., 2006; Delair, Meunir, Flaissari, Charles, & Pichot, 1999) and kits for immunoassays.

Lectins are proteins that react with specific terminal sugar residues and are useful probes in studying carbohydrates of cell surfaces (Gilboa-Garber, Mymon, & Oren, 1998; Touhami, Hoffman, Vasella, Denis, & Dufrêne, 2003b). Concanavalin A, Con A, is a model legume lectin mainly obtained from Jack Bean that can bind specifically to mannoses and glucoses segments of carbohydrates in the presence of Mn^{2+} and Ca^{2+} (Bhattacharyya, Brewer,

---

* Corresponding author. Tel.: +55 11 30913831.
  E-mail address: dfsp@iq.usp.br (D.F.S. Petri).

Brown, & Koenig, 1985; Brewer, Brown, & Koenig, 1983; Reeke, Becker, & Edelman, 1975). Recently much effort has been devoted to understand the assembling of Con A onto solid substrates and the potential applications of such assemblies. Surface plasmon resonance (SPR) studies (Smith et al., 2003) on the Con A–mannose interaction yielded the adsorption constant (K_{ads}) of 5.6×10^6 $(mol/L)^{-1}$. The adsorption constant of Con A onto carboxymethyl cellulose (CMC) films (Castro & Petri, 2005) was determined as 2.1×10^6 $(mol/L)^{-1}$. These findings showed that the affinity of Con A for glucose residues is similar to that for mannose residues. Force measurements have been used to quantify the adhesion forces between modified Con A and yeast cells (Revell et al., 1998; Gad et al., 1997), carbohydrates (Barbucci et al., 2005) and sugar residues at the surface of fibroblast cells (Chen & Moy, 2000). Traces of mannose could be detected by adhesion forces measurements between CMC hybrid particles and Con A films supported on Si wafers (Castro et al., 2006).

Cashew gum (CG) is an exudate polysaccharide from *Anacardium occidentale* trees and has been previously characterized (De Paula & Rodrigues, 1995; De Paula, Heatley, & Budd, 1998). It is a low viscosity gum, in comparison to arabic gum, which contains galactose (72%), glucose (14%) arabinose (4.6%), rhamnose (3.2%) and glucuronic acid (4.7%). Rheological properties of cashew gums has been well-reported (Zakaria & Rahman, 1996). CG is mainly composed of three types of galactan units within the core, linked by C-1 and C-3; C-1 and C-6 and C-1, C-3 and C-6. The glucose is present as sides chains, with up to 5 U long (De Paula et al., 1998). Some application based on CG has been proposed in last few years, such as superabsorbent hydrogel for soil conditioner (Guilherme et al., 2005) or polyelectrolyte complex with chitosan for drug delivery (Maciel, de Paula, Paula, Miranda, & Sassaki, 2006). CG has also been modified by carboxymethylation with monochloroacetic as etherifying agent (Silva et al., 2004).

The aim of this work is to study the adsorption behavior of CG, a galactose-rich polysaccharide, onto silicon wafers or amino-terminated surfaces by means of ellipsometry, atomic force microscopy and contact angle measurements. The immobilization of Con A, which is known to bind specifically to mannoses and glucoses segments of carbohydrates, onto CG films was also investigated.

2. Experimental

2.1. Materials

Crude samples from cashew gum (CG) were collected from native trees in Fortaleza, Ceará, Brazil. They were purified as a sodium salt using the method described elsewhere (De Paula & Rodrigues, 1995; De Paula, Santana, & Rodrigues, 2001). Nodules free of bark were selected and dissolved in distilled water at room temperature to give

a 5% solution. The solution pH was adjusted to approximately 7.0 by addition of diluted aqueous NaOH. The clear solution was successively filtered through sintered glass and the polysaccharide precipitated with ethanol. M_w 32,000 g/mol was estimated by gel permeation chromatography (GPC) at room temperature using an Ultrahydrogel linear (7.8×300 mm) column and 0.1 M $NaNO_3$ as solvent, using pullulan as standard. A differential refractometer was used as detector. CG structure is available as supplementary material.

Con A, type IV, from *Concanavalia ensiformis*, purchased from Sigma (molecular weight = 25583 g mol^{-1}), isoelectric point at 4.5–5.6 ([www.expasy.org. ID: P02866 accessed in December 2006], C2010, St. Louis, USA) was used without any purification. Con A solutions were prepared in the concentration range of 0.001–0.5 g/L at pH 4.5 or pH 6.0, in the presence of $MnCl_2$ 0.01 mol L^{-1} and $CaCl_2$ 0.01 mol L^{-1}.

Silicon (100) wafers purchased from Crystec (Berlin, Germany) were used as substrates. They were rinsed in a standard manner (Petri et al., 1999a, Petri, Wenz, Schunk, & Schimmel, 1999b). Si wafers were also modified by reacting with aminopropyltrimethoxy silane (APS, Acros, USA) (Petri et al., 1999a, 1999b). The resulting amino-terminated substrates became cationic at pH ~ 4.0.

For the adsorption experiments solutions of cashew gum (CG) were prepared in NaCl 0.1, 0.01 and 0.001 mol/L, in the concentration range of 0.01 g/L (or 0.31 μmol/L) to 1.0 g/L (or 31.2 μmol/L), at 25 °C. The medium pH was set at pH 6.0 or pH 4, for adsorption experiments of CG onto Si wafers or amino-terminated wafers, respectively.

CG-coated substrates were immersed for 3 h, at 25 °C, in aqueous solutions of Con A prepared in the concentration range of 0.001 g/L (or 0.04 μmol/L) to 0.5 g/L (or 19.5 μmol/L) in the presence of $MnCl_2$ 0.01 mol/L and $CaCl_2$ 0.01 mol/L. The medium pH was adjusted at pH 6.0 or pH 4.5, when the substrates used were CG-covered Si wafers or CG-covered amino-terminated wafers, respectively.

2.2. Ellipsometry

Ellipsometric measurements were performed *ex situ* using a vertical computer-controlled DRE-EL02 Ellipsometer (Ratzeburg, Germany). The angle of incidence was set to 70.0° and the wavelength of the laser was 632.8 nm with an incidence area of 3 mm². For the interpretation of the ellipsometric angles Δ and Ψ a multilayer model was used, assuming refractive index n for Si, 3.88–0.018i; for SiO_2, 1.462; for polysaccharide layer, 1.500, for the bulk solution 1.333, as measured by Abbé refractometer, and for air 1.000. If the adsorbed polysaccharide layer is regarded as a homogeneous film, the thickness can be calculated by iterative calculations with Jones matrices (Azzam & Bashara, 1987; Motschmann, Stamm, & Toprakcioglu, 1991). Each layer is usually characterized sequentially regarding independent ellipsometric determinations of thickness and

refractive index (Azzam & Bashara, 1987; Motschmann et al., 1991). One should also notice that ellipsometry enables the independent determination of n and d, only if the optical contrast in the system is large enough or if the layer thickness is thick enough. When λ is 633 nm and $d \gg 30$ nm, it is possible to obtain n and d for the uppermost layer independently. However, in the present system, $d \ll 30$ nm for the uppermost polymer layer, so that n must be assumed as $n = 1.500$, the usual value for a polysaccharide layer, and d calculated from ellipsometric angles and the multilayer model plus independent determinations of thicknesses and refractive indices for each layer.

The surface coverage Θ was calculated dividing the thickness d measured at a given CG concentration and the thickness at limiting adsorption d_{max}:

$$\Theta = \frac{d}{d_{max}} \tag{1}$$

The dependence of Θ on CG concentration could be described by the Langmuir adsorption model (Adamson, 1990):

$$\Theta = \frac{K_{ads} \cdot C_{CG}}{(1 + K_{ads} \cdot C_{CG})} \tag{2}$$

where C_{CG} is the concentration of CG in solution and K_{ads} is the adsorption constant. The larger is K_{ads} the higher is the affinity between substrate and adsorbate.

The adsorption of Con A onto polysaccharide-coated substrates was monitored by means of ellipsometry. The thickness of Con A layer was calculated, considering the refractive index of 1.520 a typical value for proteins (Malmsten, 2000).

2.3. Atomic force microscopy (AFM)

AFM topographic images were obtained using a PicoSPM-LE Molecular Imaging system with cantilevers operating in the intermittent-contact mode (AAC mode), slightly below their resonance frequency of approximately 290 kHz in the air. All topographic images represent unfiltered original data and refer to scan areas of 1×1 μm. At least two samples of the same material were analyzed at different areas of the surface. Image processing and the determination of the root mean square (rms) roughness were performed by using the PicoScan 5.3.2. software.

2.4. Contact angle measurements

Contact angle measurements were performed in a home-built apparatus (Adamson, 1990) equipped with a digital camera, which is connected to a computer. Sessile water drops of 8 and 4 μL were used for advancing (θ_A) and receding (θ_R) angle, respectively. The hysteresis in the contact angle ($\Delta\theta = \theta_A - \theta_R$) stems from surface roughness or surface chemical heterogeneities (Adamson, 1990).

3. Results and discussion

3.1. Adsorption of CG onto Si wafers or amino-terminated substrates

The interactions between substrate and polyelectrolytes can be strongly influenced by ionic strength, segment charge and surface charge. CG chains behave as polyanions at pH > 4.0 due to the presence of glucuronic acid (p$K_a \sim 3.5$) functionalities (4.7%). The degree of dissociation depends on pH and electrolyte concentration. At pH 4.0 CG chains are negatively charged, while the amino-terminated surface is highly protonated (Fujimoto & Petri, 2001). Fig. 1 shows mean layer thickness (d) values of adsorbed CG onto amino-terminated surfaces as a function of CG concentration under different ionic strengths. The mean thickness values obtained at 0.001 (circles) and 0.01 mol/L (squares) NaCl were similar, regardless the CG concentration. Upon increasing the ionic strength to 0.1 mol/L NaCl (triangles) the mean thickness values decreased considerably. This behavior indicates that the adsorption of CG onto amino-terminated surfaces is mainly driven by electrostatic forces, since salt screens not only the segment–segment repulsion but also the segment–surface attraction when salt concentration increases, following the screening-reduced adsorption regime (Hoogendam et al., 1998). Such behavior has also been observed for the adsorption of carboxymethylcellulose onto amino-terminated surfaces (Fujimoto & Petri, 2001).

Considering the CG mean thickness value at limiting adsorption d_{max} obtained in 0.01 mol/L NaCl as (2.1 ± 0.2) nm (Fig. 1), the surface coverage values Θ were calculated as function of CG concentration (Fig. 2). The data could be fitted by the Langmuir adsorption model, with K_{ads} value of $(2.5 \pm 0.2) \times 10^5$ L mol^{-1}.

The adsorption behavior of CG onto Si wafers was investigated at pH 6.0 and 0.001 mol/L NaCl. The mean thickness of adsorbed CG layers onto Si wafers at pH 6.0
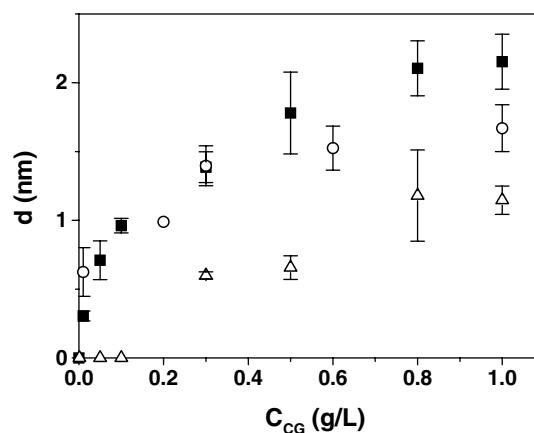

Fig. 1. Mean thickness of adsorbed CG layer onto amino-terminated surfaces as a function of CG concentration at pH 4, in (○) 0.001 mol/L, (■) 0.01 mol/L and (△) 0.1 mol/L NaCl, after 3 h of adsorption.
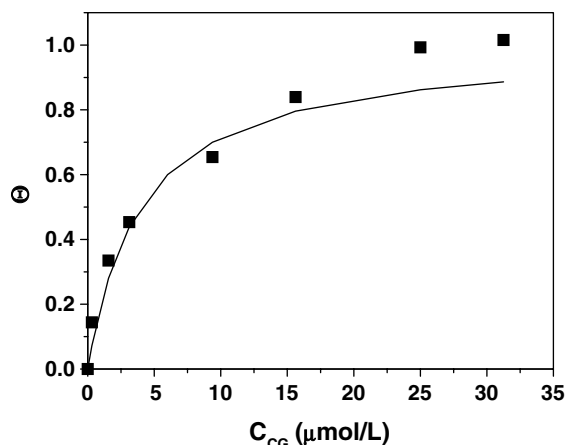
Fig. 2. Dependence of surface coverage Θ on CG concentration determined from mean thickness of adsorbed CG layer onto amino-terminated at pH 4 in 0.01 mol/L NaCl (solid squares in Fig. 1). The solid line represents the fit according to Langmuir adsorption model.
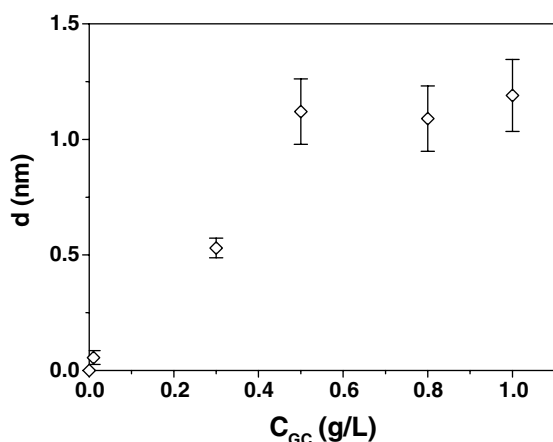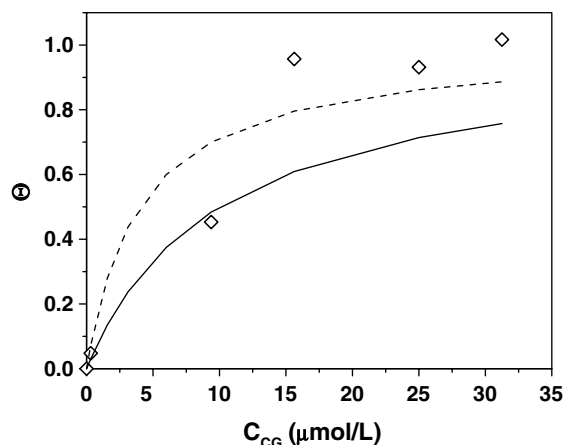

Fig. 4. Dependence of surface coverage Θ on CG concentration determined from mean thickness of adsorbed CG layer onto Si wafers at pH 6 in 0.001 mol/L NaCl (open diamonds in Fig. 3). The solid and dashed lines represent the fit according to Langmuir adsorption model considering $K_{ads} = 1.0 \times 10^5$ L/mol and $K_{ads} = 2.5 \times 10^5$ L/mol, respectively.

Fig. 3. Mean thickness of adsorbed CG layer onto Si wafers as a function of CG concentration at pH 6, in 0.001 mol/L NaCl, after 3 h of adsorption.

(Si–OH and Si–O$^-$) are exposed to the adsorbate. Langmuir adsorption model assumes that all binding sites have the same adsorption energy, and that is not the actual situation.

Table 1 presents θ_A, θ_R and $\Delta\theta$ values determined for water drops onto original substrates and CG covered substrates. The wettability of Si wafers and amino-terminated surfaces decreased upon adsorbing CG. However, the mean θ_A values obtained for CG adsorbed onto both substrates of $\sim 32°$ indicate very hydrophilic surfaces. This hydrophilic nature is due to the hydroxyl (–OH) rich CG structure. $\Delta\theta$ values determined for CG adsorbed onto both substrates are similar.

CG layers formed onto amino-terminated wafers presented morphological features distinct from those observed for CG layers adsorbed onto Si wafers, as revealed by AFM. Fig. 5a shows a typical topographic image of CG onto amino-terminated substrate with the corresponding cross section (Fig. 5b). CG layer onto amino-terminated substrate is flat (rms = 0.26 ± 0.05 nm, Table 1) and composed of fine structures well distributed over the substrate. Fig. 6a shows a typical topographic image of CG layers onto Si wafer. CG film formed onto Si wafer is also smooth (rms = 0.18 ± 0.03 nm, Table 1), but thinner than the CG films formed onto amino-terminated wafers, as evidenced by the corresponding cross section (Fig. 6b). These findings corroborate with the adsorption isotherms presented in Figs. 1–4.

3.2. Adsorption of concancavalin A onto CG covered substrates

The adsorption behavior of Con A onto CG-covered amino-terminated substrates at pH 4.5 was distinct form that observed for Con A onto CG-covered Si wafers at pH 6.0, as shown in Fig. 7.

as a function of CG concentration is shown in Fig. 3. Comparing these data with those presented in Fig. 1, one observes that the adsorption of CG onto Si wafers is less favored than onto amino-terminated surfaces. This might be due to the substrate charge. At pH 6.0 Si wafers presents not only silanol groups (Si–OH) but also many negative charges (Si–O$^-$), which repel the negatively charged CG segments (carboxylate groups). On the other hand, hydrogen bonding between silanol groups and sugar hydroxyl groups might drive the adhesion of CG onto Si wafers, when the CG concentration is higher than 0.2 g/L. Fig. 4 shows the surface coverage values Θ calculated as function of CG concentration, considering the CG mean thickness value at limiting adsorption d_{max} as (1.1 ± 0.1) nm (Fig. 3). The data did not fit well the Langmuir adsorption model, assuming K_{ads} value of $(2.5 \pm 0.2) \times 10^5$ L mol^{-1} or $(1.0 \pm 0.1) \times 10^5$ L mol^{-1}. One possible reason for the lack of fit might be the chemically heterogeneous nature of Si wafers at pH 6.0, where two kinds of binding sites

Table 1
Advancing (θ_A) and receding (θ_R) contact angle measurements, respectively, and rms values

Sample	θ_A (°)	θ_R (°)	$\Delta\theta$ (°)	Rms (nm)
Si wafer	5	–	–	0.10 ± 0.02
Amino-terminated substrate	23 ± 2	19 ± 2	4 ± 2	0.15 ± 0.03
CG onto Si wafer (pH 6.0)	32 ± 2	19 ± 2	13 ± 2	0.18 ± 0.03
CG onto amino-terminated substrate (pH 4.0)	34 ± 2	22 ± 2	12 ± 2	0.26 ± 0.05
Con A onto CG covered Si wafer (pH 6.0)	47 ± 4	28 ± 3	19 ± 4	0.67 ± 0.09
Con A onto CG covered amino-terminated wafer (pH 4.0)	55 ± 5	38 ± 4	17 ± 5	0.87 ± 0.08

The hysteresis in the contact angle $\Delta\theta$ was calculated from $\Delta\theta = \theta_A - \theta_R$.
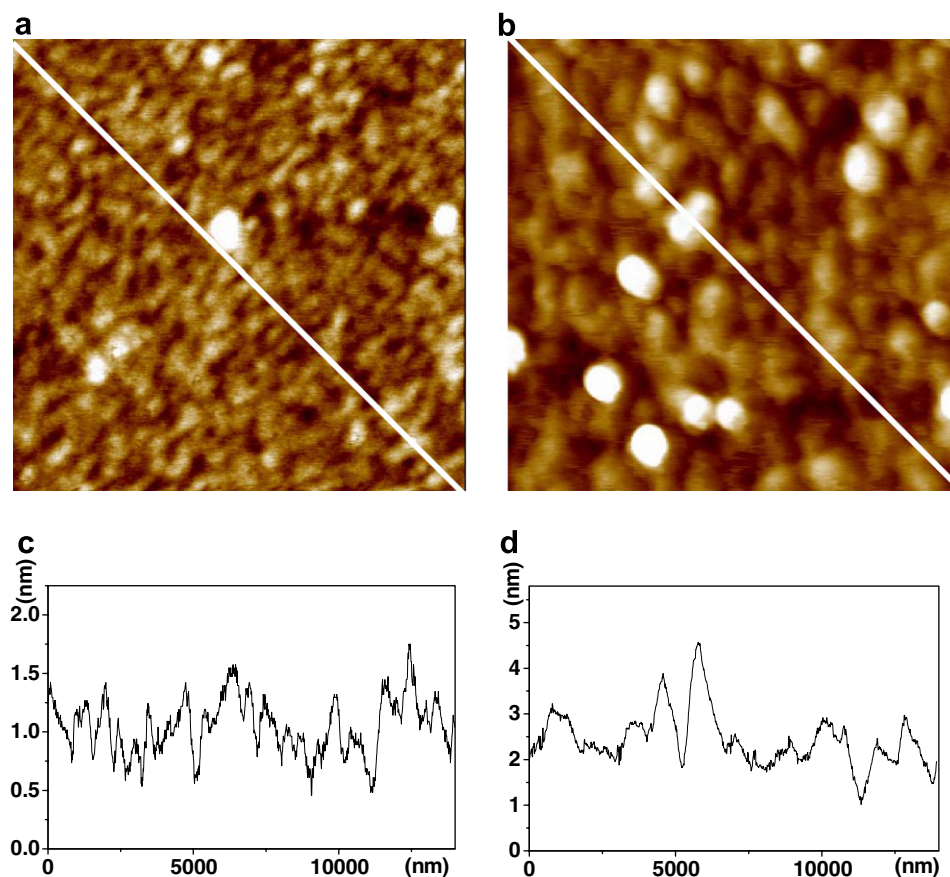

Fig. 5. Topographic images obtained by means of AFM intermittent contact in the air for (a) CG adsorbed onto amino-terminated surfaces from a 0.3 g/L solution ($Z = 20$ nm) (b) for Con A adsorbed onto CG covered amino-terminated substrates from a 0.1 g/L solution (or 3.9 μmol/L) ($Z = 50$ nm). Scan areas of 1×1 μm. Cross sections (c) and (d) correspond to the topographic images (a) and (b), respectively, as indicated by the solid lines.

The adsorption of Con A onto CG-covered Si wafers at pH 6.0 (open squares) led to mean d values of Con A, which increased with Con A concentration up to approximately (3.0 ± 0.2) nm at 0.2 g/L (or 7.8 μmol/L) of Con A, the adsorption plateau onset. The dependence of surface coverage Θ (calculated considering Eq. (1) and d_{max} of 3.0 nm) with Con A concentration could be fitted with the Langmuir adsorption model with K_{ads} $(2.0 \pm 0.2) \times 10^6$ L mol^{-1} (Fig. 8). This value is identical with that found for the adsorption of Con A onto carboxymethylcellulose covered surface (Castro & Petri, 2005) and similar to that determined for Con A adsorbing onto a mannose surface

(Smith et al., 2003). This is a very interesting finding because CG is galactose rich, and has shown strong affinity for specific proteins such as frutalin and jacalin (lectins from Artocarpus seeds) (Lima, Lima, Salis, & Moreira, 2002). This behavior might be explained by the presence of glucose (14%) (De Paula et al., 1998) as side-chain, which favors the interaction with Con A. Spectroscopic studies (Revell et al., 1998) revealed that the molecular recognition of Con A for mannose and glucose residues stems from these carbohydrates possessing hydroxyl configurations at the 3, 4 and 6 carbons. This result suggests that the strong affinity of Con A for glucose does not depend
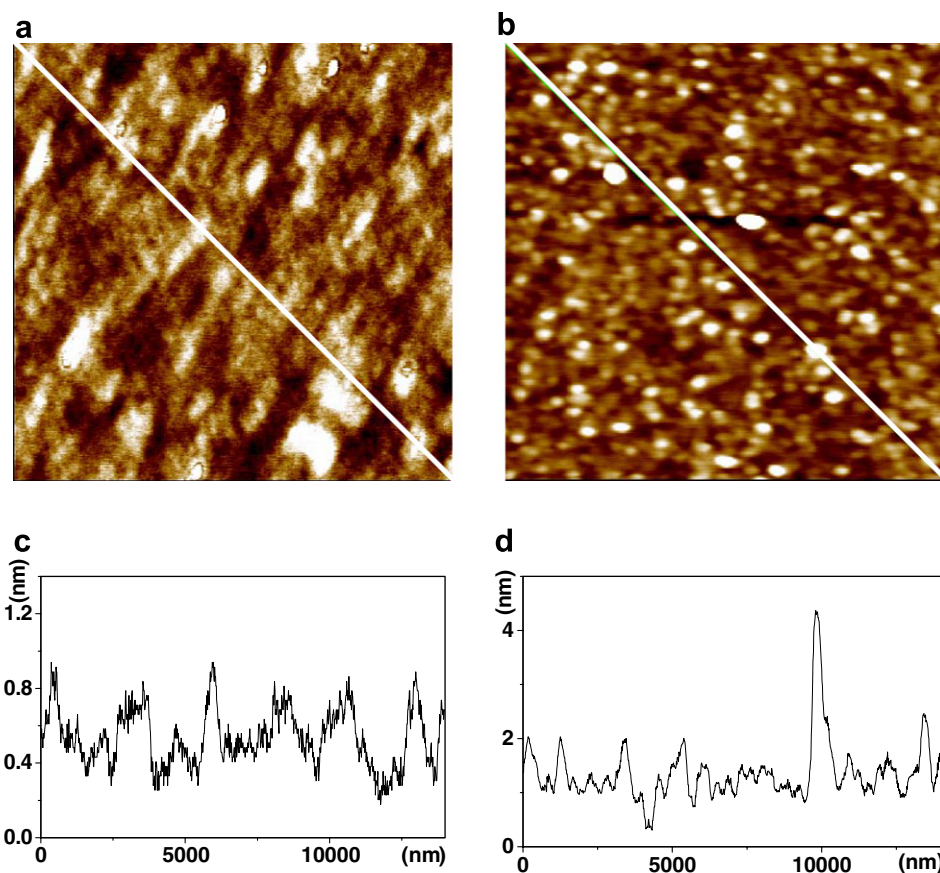
Fig. 6. Topographic images obtained by means of AFM intermittent contact in the air for (a) CG adsorbed onto Si wafers from a 0.3 g/L solution ($Z = 10$ nm) (b) for Con A adsorbed onto CG covered Si wafers from a 0.001 g/L (or 0.04 μmol/L) solution ($Z = 30$ nm). Scan areas of 1×1 μm. Cross sections (c) and (d) correspond to the topographic images (a) and (b), respectively, as indicated by the solid lines.
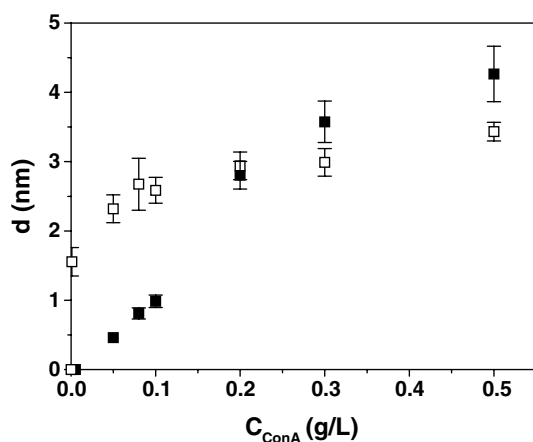

Fig. 7. Mean thickness of adsorbed Con A onto CG covered amino-terminated substrates at pH 4.0 (■) or onto CG covered Si wafers pH 6.0 (□) as a function of CG concentration, after 3 h of adsorption.
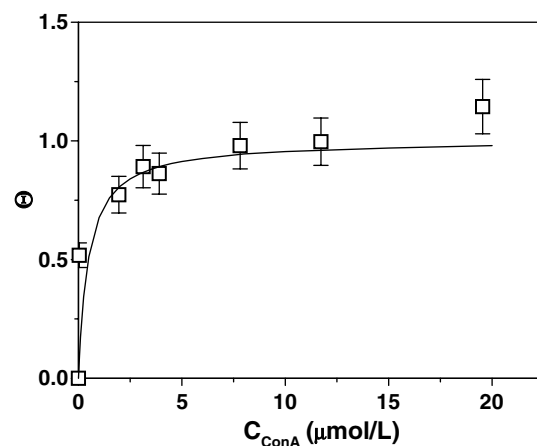
Fig. 8. Dependence of surface coverage Θ on Con A concentration determined from mean thickness of Con A adsorbed onto CG covered Si wafers at pH 6 (open square in Fig. 7). The solid line represents the fit according to Langmuir adsorption model considering $K_{ads} = 2.1 \times 10^6$ L/mol.

only on the amount glucose or mannose units present in the polysaccharide, but also as the monomers units are available for its specific sites.

The topographic features of CG-covered Si wafers changed considerably after the adsorption of Con A, as shown in Fig. 6c and d. The surface became rougher (rms $= 0.67 \pm 0.09$ nm) and presented small spherical entities ~4.5 nm high, which were attributed to assembled Con A molecules. Similar features have been already observed

for Con A adsorbed onto CMC films (Catro & Petri, 2005; Castro et al., 2006), creatine phosphokinase (Pancera, Gliemann, Schimmel, & Petri, 2006) or enolase (Almeida, Salvadori, & Petri, 2002) or human serum albumin, immunoglobulin G (IgG) and fibrinogen (Ortega-Vinuesa, Tengvall, & Lundstöm, 1998) onto silicon wafers. Upon drying lateral diffusion of the adsorbed proteins and lateral interactions among the proteins might lead to clustering on the surface.

The mean thickness values d of Con A layer formed onto CG covered amino-terminated substrates increased as a function of Con A concentration. No equilibrium plateau could be observed. The continuously increase of d indicates a cooperative adsorption process, which is commonly observed for proteins. Con A films are formed by densely packed entities (Fig. 5c) with heights varying from 3 to 4.5 nm and the substrate seems to be completely covered, as evidenced by the cross section in Fig. 5d. After the adsorption of Con A the surface roughness increased significantly from 0.26 ± 0.05 to 0.87 ± 0.08 nm (Table 1).

Upon adsorbing Con A onto CG-covered Si wafers or onto CG-amino-terminated substrates the θ_A values shown in Table 1 increased up to $(55 \pm 5°)$, indicating the exposition of some Con A hydrophobic residues to the air. Similar behavior has been observed for Con A onto CMC and Si wafers (Castro & Petri, 2005), creatine phosphokinase (Pancera et al., 2006) or enolase (Almeida et al., 2002) onto Si wafers.

4. Conclusions

CG, a polysaccharide composed of galactose (72%), glucose (14%) arabinose (4.6%), rhamnose (3.2%) and glucuronic acid (4.7%), adsorbed onto amino-terminated surfaces under pH 4 due to electrostatic interactions. The adsorbed amount decreased with ionic strength, in agreement with the screening-reduced adsorption regime. Under pH 6 (or pH 4) the adsorption of CG onto bare Si wafers was less favored, indicating that silanol groups (Si–OH) and many negative charges (Si–O⁻) on the substrate repel the negatively charged CG segments. In that case hydrogen bonding between silanol groups and sugar hydroxyl groups might drive the adhesion of CG onto Si wafers. Regardless the substrate nature, smooth and hydrophilic CG layers were observed. These layers formed attractive surfaces for the immobilization of Con A. Under pH 4 the adsorption of Con A onto CG-covered amino-terminated substrates increased with Con A concentration, evidencing cooperativity. Under pH 6 the adsorption isotherm of Con A onto CG coverd Si wafers could also be fitted, obtaining adsorption constant of 2.1×10^6 L/mol, which is similar to values found for the adsorption of Con A onto carboxymethylcellulose or mannose films. The strong affinity of Con A for glucose seems to depend not only on the amount glucose or mannose units present in the polysaccharide, but also as the monomers units are available for its specific sites.

CG presents 14% of glucose as side-chains, which are free to interact with Con A.

References

Adamson, W. A. (1990). *Physical chemistry of Surfaces* (5th ed.). Toronto: John Wiley and Sons.

Almeida, A. T., Salvadori, M. C., & Petri, D. F. S. (2002). Enolase adsorption onto hydrophobic and hydrophilic solid substrates. *Langmuir, 18*(18), 6914–6920.

Azzam, R. M. A., & Bashara, N. M. (1987). *Ellipsometry and polarized light*. Amsterdan: North Hollan Publication.

Barbucci, R., Magnani, A., Chiumiento, A., Pasqui, D., Cangioli, I., & Lamponi, S. (2005). Fibroblast cell behavior on bound and adsorbed fibronectin onto hyaluronan and sulfated hyaluronan substrates. *Biomacromolecules, 6*(2), 638–645.

Bhattacharyya, L., Brewer, C., Brown, S., & Koenig, S. (1985). Proton and deuteron nuclear magnetic relaxation dispersion studies of calcium(2+)–manganese(2+)-lentil lectin and calcium(2+)–manganese(2+)-pea lectin: evidence for a site of solvent exchange in common with concanavalin A. *Biochemistry, 24*(19), 4985–4990.

Brewer, C. F., Brown, R. D., & Koenig, S. H. (1983). Stoichiometry of magnesium and calcium ion binding to concanavalin A. *Biochemistry, 22*(15), 3691–3702.

Castro, L. B. R., & Petri, D. F. S. (2005). Assemblies of Concanavalin A onto carboxymethylcellulose. *Journal of Nanoscience and Nanotechnology, 5*(12), 2063–2069.

Castro, L. B. R., Kappl, M., & Petri, D. F. S. (2006). Adhesion forces between hybrid colloidal particles and Concanavalin A. *Langmuir, 22*(8), 3757–3762.

Chen, A., & Moy, V. T. (2000). Cross-linking of cell surface receptors enhances cooperativity of molecular adhesion. *Biophysical Journal, 78*(6), 2814–2820.

De Paula, R. C. M., & Rodrigues, J. F. (1995). Composition and rheological properties of cashew tree gum, the exudate polysaccharide from Anacardium occidentale L. *Carbohydrate Polymers, 26*(3), 177–181.

De Paula, R. C. M., Heatley, F., & Budd, P. M. (1998). Characterization of Anacardium occidentale exudate polysaccharide. *Polymer International, 4*(1), 27–35.

De Paula, R. C. M., Santana, S. A., & Rodrigues, J. F. (2001). Composition and rheological properties of Albizia lebbeck gum exudate. *Carbohydrate Polymers, 44*(2), 133–139.

Delair, T., Meunir, F., Flaissari, A., Charles, M.-H., & Pichot, C. (1999). Amino-containing cationic latex-oligodeoxyribonucleotide conjugates: application to diagnostic test sensitivity enhancement. *Colloids and Surfaces A: Physicochemical and Engineering Aspects, 153*(1–3), 341–353.

Fujimoto, J., & Petri, D. F. S. (2001). Adsorption behavior of carboxymethylcellulose on amino-terminated surfaces. *Langmuir, 17*(1), 56–60.

Fujimoto, J., Reis, E. A. D., Petri, D. F. S., & Campana, S. P. (2002). Formation of polysaccharides and protein multilayers. *Quimica Nova, 25*(5), 757–761.

Gad, M., Ioth, A., & Ikai, A. (1997). Mapping cell wall polysaccharides of living microbial cells using atomic force microscopy. *Cell Biology International, 21*(11), 697–706.

Gilboa-Garber, N., Mymon, H., & Oren, A. (1998). Typing of halophilic Archaea and characterization of their cell surface carbohydrates by use of lectins. *FEMS Microbiology Letters, 163*(1), 91–97.

Guilherme, M. R., Reis, A. V., Takahashi, S. H., Rubira, A. F., Feitosa, J. P. A., & Muniz, E. C. (2005). Synthesis of a novel superabsorbent

hydrogel by copolymerization of acrylamide and cashew gum modified with glycidyl methacrylate. *Carbohydrate Polymers, 61*(4), 464–471.

Hoogendam, C. W., de Keizer, A., Cohen Stuart, M. A., Bijster-bosh, B. H., Batelaan, J. G., & van der Horst, P. M. (1998). Adsorption mechanisms of carboxymethyl cellulose on mineral surfaces. *Langmuir, 14*(14), 3825–3839.

Lekka, M., Laider, P., Dulinska, J., Labedz, M., & Pyka, G. (2004). Probing molecular interaction between concanavalin A and mannose ligands by means of SFM. *The European Biophysics Journal, 33*(7), 644–650.

Lima, R. S. N., Lima, J. R., Salis, C. R., & Moreira, R. A. (2002). Cashew-tree (Anacardium occidentale L.) exsudate gum: a novel bioligand tool. *Biotechnology and Applied Biochemistry, 35*, 45–53.

Maciel, J. S., de Paula, R. C. M., Paula, H. C. B., Miranda, M. A. R., & Sassaki, J. M. (2006). Reacetylated chitosan/cashew gum gel: preliminary study for potential utilization as drug release matrix. *Journal of Applied Polymer Science, 99*(1), 326–334.

Malmsten, M. (2000). Protein adsorption at the solid-liquid interface. In Y. Lvov & H. Möhwald (Eds.), *Protein Architecture: Interfacing Molecular Assemblies and Immobilization Biotechnology* (pp. 1–23). New York: Marcel Dekker.

Motschmann, H., Stamm, M., & Toprakcioglu, C. (1991). Adsorption kinetics of block copolymers from a good solvent: a two-stage process. *Macromolecules, 24*(12), 3681–3688.

Ortega-Vinuesa, J. L., Tengvall, P., & Lundstöm, I. (1998). Molecular packing of HSA, IgG, and fibrinogen adsorbed on silicon by AFM imaging. *Thin Solid Films, 324*(1,2), 257–273.

Pancera, S. M., Gliemann, H., Schimmel, T., & Petri, D. F. S. (2006). Effect of pH on the adsorption and activity of creatine phosphokinase. *The Journal of Physical Chemistry B, 110*(6), 2674–2680.

Petri, D. F. S., Choi, S. W., Beyer, H., Schimmel, Th., Bruns, M., & Wenz, G. (1999a). Synthesis of a cellulose thiosulfate and its immobilization on gold surfaces. *Polymer, 40*(6), 1593–1601.

Petri, D. F. S., Wenz, G., Schunk, P., & Schimmel, T. (1999b). An improved method for the assembly of amino-terminated monolayers on SiO$_2$ and the vapor deposition of gold layers. *Langmuir, 15*(13), 4520–4523.

Reeke, G. N., Jr., Becker, J. W., & Edelman, G. M. (1975). The covalent and three-dimensional structure of concanavalin A. III. Structure of the monomer and its interactions with metals and saccharides. *The Journal of Biological Chemistry, 250*(4), 1513–1524.

Revell, D. J., Knight, J. R., Blyth, D. J., Haines, A. H., & Russel, D. A. (1998). Self-assembled carbohydrate monolayers: formation and surface selective molecular recognition. *Langmuir, 14*(16), 4517–4524.

Sackmann, E. (1996). Supported membranes: scientific and practical applications. *Science, 271*(5245), 43–48.

Sierakowski, M. R., Freitas, R. A., Fujimoto, J., & Petri, D. F. S. (2002). Adsorption behavior of oxidized galactomannans onto amino-terminated surfaces and their interaction with bovine serum albumin. *Carbohydrate Polymers, 49*(2), 167–175.

Silva, D. A., de Paula, R. C. M., Feitosa, J. P. A., de Brito, A. C. F., Maciel, J. S., & Paula, H. C. B. (2004). Carboxymethylation of cashew tree exudate polysaccharide. *Carbohydrate Polymers, 58*(2), 163–171.

Smith, E. A., Thomas, W. D., Kiessling, L. L., & Corn, R. M. (2003). Surface plasmon resonance imaging studies of protein–carbohydrate interactions. *Journal of the American Chemical Society, 125*(20), 6140–6148.

Touhami, A., Hoffman, B., Vasella, A., Denis, F. A., & Dufrêne, Y. F. (2003a). Probing specific lectin–carbohydrate interactions using atomic force microscopy imaging and force measurements. *Langmuir, 19*(5), 1745–1751.

Touhami, A., Hoffman, B., Vasella, A., Denis, F. A., & Dufrêne, Y. F. (2003b). Aggregation of yeast cells: direct measurement of discrete lectin–carbohydrate interactions. *Microbiology, 149*(10), 2873–2878.

Wiegand, G., Jaworek, T., Wegner, G., & Sackmann, E. (1997). Heterogeneous surfaces of structured hairy-rod polymer films: preparation and methods of functionalization. *Langmuir, 13*(13), 3563–3569.

Zakaria, M. B., & Rahman, Z. A. (1996). Rheological properties of cashew gum. *Carbohydrate Polymers, 29*(1), 25–27.